geoconvention
Virtual Event
September 21-23
2020
CSPG • CSEG • CWLS • GAC • MAC • IAH

Incorporating time shifts and rock physics for model updates in 4D inversion

Carl Reine, Draga Talinga Sound QI Solutions Ltd.
Liliana Zuleta, Mike Palka CNOOC International Ltd.

Summary

In time-lapse (4D) seismic analysis, extending the interpretation to include AVO inversion provides valuable information. Changes in elastic properties of the reservoir help build a quantitative understanding of the changes in temperature, pressure, and fluids. To properly measure the time-lapse elastic property changes in a thick zone, such as those encountered in SAGD operations, we demonstrate why appropriate changes to the initial model must be performed for the monitor inversion. By incorporating the time shifts obtained in the calibration of the baseline and monitor surveys, we show the process to calculate explicit changes for some of the model parameters. To complete the process, we also incorporate rock-physics modelling, improving the process from assumptions that must otherwise be made. Using two case studies, we show how the rock-physics modelling is used to further interpret the results and produce volumes that readily display reservoir changes.

Method

4D Differences in seismic traveltimes and amplitudes caused by changes in the reservoir conditions are useful for mapping the affected areas. By performing AVO inversion on the 4D survey, these changes can be quantified in terms of temperature, pressure, and saturation changes.

A key component of inversion is the initial model, providing the starting point from which the inversion converges to a final result. Updating these models when the reservoir properties have changed significantly over a thick interval (affecting the low-frequency component), is a key consideration for 4D inversion. The inversion results when the models are not updated still indicated the presence of reservoir changes, however the magnitudes are inconsistent and artifacts outside of the reservoir are produced. Specifically, in the context of the Alberta oil sands, the thick nature of the McMurray reservoir and the large property changes brought about by SAGD operations necessitate this model update.

A variety of methods have been used to update the initial models. These include interpretive methods (Mesdag et al., 2015), scaling the models based on horizon shifts (Gray et al., 2016), and the use of the time shift measured between the baseline and monitor surveys (Nasser et al., 2016; Mutual et al., 2017; Maleki et al., 2018).

The method used here incorporates the volumetric time shifts derived by aligning the monitor survey with the baseline reflections. This is a necessary step for direct comparison of amplitude and inversion differences and requires no additional interpretation. Assuming that there is negligible change in depth (i.e. from geomechanical compaction or uplift), the time difference from PP data can be translated directly into changes in P-wave velocity, which along with density are the components of P-impedance. The interval P-wave monitor velocity v_{Pmon} can be shown to be equal to

$$v_{Pmon} = v_{Pbase}\left(\frac{t_{ibase}}{t_{ibase}+\Delta t_i}\right),$$

where v_{Pbase} is the interval P-wave velocity for the baseline survey, t_{ibase} is the baseline P-wave traveltime within the interval, and Δt_i is the interval P-wave time difference between the monitor and baseline traveltimes. This update to the velocity can be calculated at each sample, allowing for the velocity modifications to be appropriately located in time.

A similar approach can be used to derive an expression for PS data that gives the updated S-wave velocity for the monitor survey as a function of P-wave and S-wave velocities and changes in PS traveltimes (Gray et al., 2016). While ideal, PS data are unfortunately not always available to perform this second update. There is also no kinematic information that can be used to update the density model, which is often assumed to remain constant for simplicity. The missing data can be approximated using rock-physics modelling that is also useful for the interpretation workflow (Nasser et al., 2016; Mutual et al., 2017).

Rock-physics models are created for a range of porosities, lithologies, and reservoir conditions expected from field development. In the expected reservoir conditions of the examples shown here, the change in density from the initial conditions was nearly linear with respect to the velocity changes. The maximum modelled shift $\Delta\rho_{max}$ is therefore scaled according to the relative traveltime shifts

$$\rho_{mon} = \rho_{base} + \frac{\Delta t_i}{\Delta t_{imax}}\Delta\rho_{max},$$

where Δt_{imax} is the maximum incremental traveltime shift.

To derive the changes in S-wave velocities, v_P:v_S ratios γ are used to convert the P-wave traveltimes. This results in an intermediate expression for the monitor interval S-wave velocity v_{Smon}:

$$v_{Smon} = v_{Sbase}\frac{\gamma_{base}}{\gamma_{mon}}\left(\frac{t_{ibase}}{t_{ibase}+\Delta t_i}\right).$$

While it is possible to use absolute values of γ for the two surveys, the amount that γ varies depends on the porosity and lithology of the reservoir. For this reason, it is more reliable to use the ratio A between the monitor and baseline γ. This ratio was calculated for the rock-physics model data, relative to the starting conditions, for the maximum injection conditions expected over the different model lithologies. The maximum expected value of A (from rock-physics modelling) is then scaled by the relative traveltime shifts:

$$\frac{1}{A} = \left(\frac{1}{A_{max}} - 1\right)\frac{\Delta t_i}{\Delta t_{imax}} + 1,$$

This function is then applied to the average velocity expression to give

$$v_{Smon} = v_{Sbase}\frac{1}{A}\left(\frac{t_{ibase}}{t_{ibase}+\Delta t_i}\right).$$

For heavy-oil scenarios, the S-wave correction is not as robust as for the density model given that it will underestimate the value of A when the bitumen is only slightly heated (resulting in an increase in γ). Nevertheless, in the absence of PS data, the approximation is better than scaling

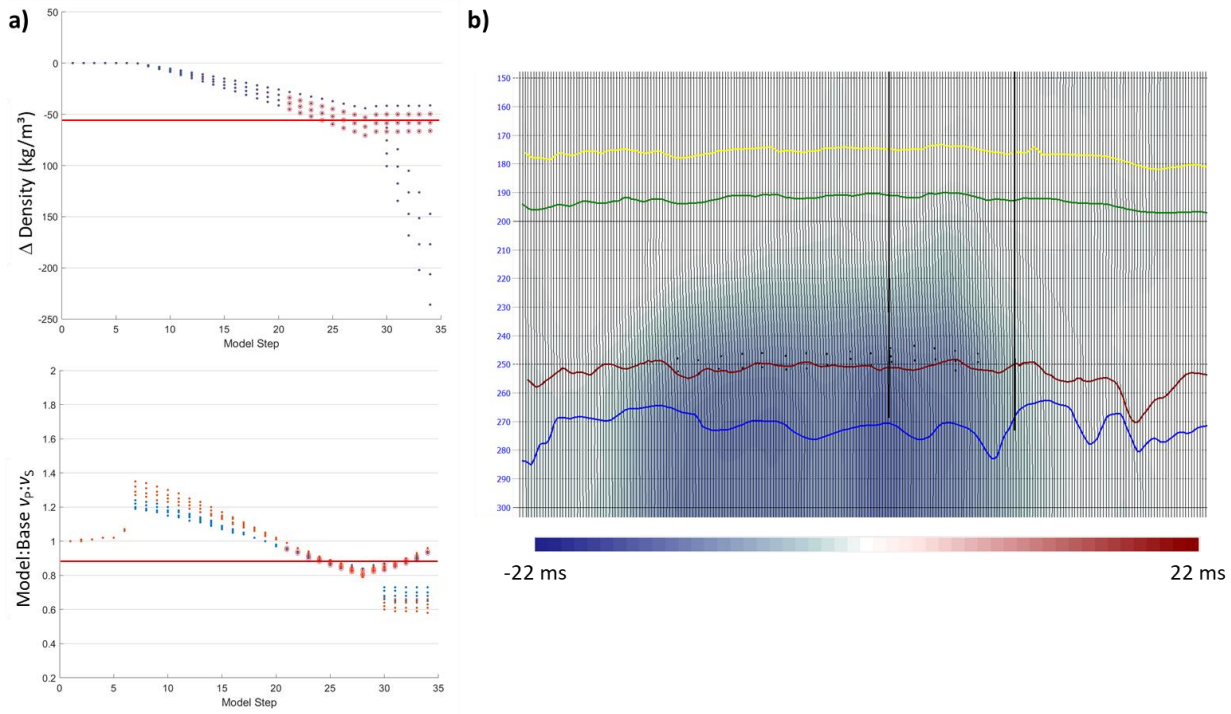

Figure 1. *a) Rock-physics model showing increase in pressure, temperature, and water saturation. The values are expressed in changes in density (top) and ratio of vP:vS, corresponding to the equations used in the model update. b) The time shift from dynamic warping between baseline and monitor surveys is used in the same equations.*

the velocities directly, as it accounts for variations in lithology through its dependence on the baseline γ.

Examples

In both examples, three main effects were considered in sequence for the rock-physics modelling. The evolution of the steam injection assumed that the pressure effects would occur first, raising the pore pressure to the operating injection pressure. Temperature effects were then introduced, from initial conditions to the maximum steam temperature. Finally, bitumen was replaced by either steam or hot water. This progression was intended to simulate the evolution of the steam flood at a given point.

A representative rock model was modelled as an unconsolidated sandstone (Dvorkin and Nur, 1996) with methodologies suitable for heavy oils (Ciz and Shapiro, 2007; Javanbakhti, 2018). Because a range of facies are present in the reservoir, each with different elastic properties, the reservoir zone included models of clean sand and IHS over a range of porosities.

For the first example, Figure 1a shows the effects of the different model steps for the change in density from baseline conditions and the ratio of v_P:v_S relative to the baseline conditions. The difference and ratio are necessary to normalize the monitor conditions across different porosities and facies. The average values for the ratio and difference are shown for the expected conditions

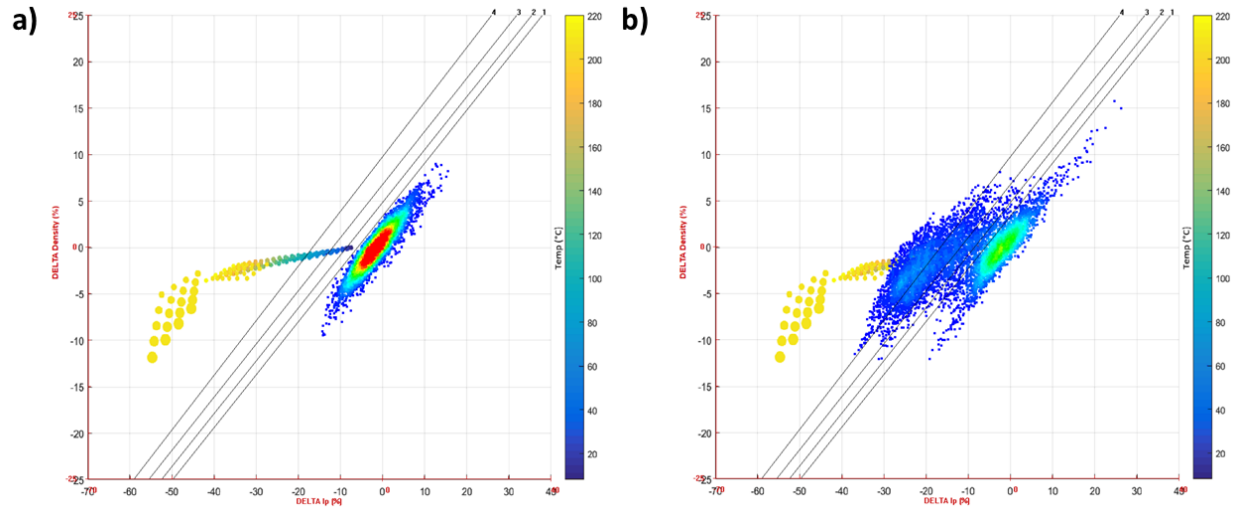

Figure 2. *Crossplot templates using rock-physics data. The colour of the large points corresponds to the modelled temperature. The point size is proportional to steam saturation. The templates are shown with seismic inversion data from areas a) outside and b) inside the steamed area.*

in the most heavily affected steamed area. In this example data, the monitor survey was acquired approximately 9.5 years after the start of steam injection, and the affected reservoir is expected to be widespread. Figure 1b shows the time-variant shifts obtained with a dynamic warping algorithm (Hale, 2013) between the baseline and monitor survey. The majority of the time shift is observed, as expected, within and below the McMurray reservoir.

The rock-physics data for steam-injection steps were arranged into a template of $\Delta\rho$ versus ΔI_P (Figure 2a). Although I_S changes significantly for initial temperature drops, I_P is useful in the context of more mature steam injections as it corresponds well to continued temperature changes. Density changes are much smaller until gas-phase steam is introduced. The presence of different facies in the model causes the points for a single 4D step to spread obliquely in the crossplot domain.

Including the inverted seismic data on this crossplot demonstrates why the use of any single attribute is not ideal for interpreting 4D response. The unchanged reservoir data (Figure 2a) has random fluctuations of time-lapse changes. Because of the inversion, P-impedance and density fluctuations are correlated, rather than random. This trend is similar, but not necessarily identical to the spread in the time-lapse changes due to porosity and facies variations. In using a single attribute, I_P in this case, changes would show erroneous information from random fluctuations or when different lithologies are present. The use of a second attribute helps solve this problem.

The data from inside the steamed area (Figure 2b) has a larger spread in the crossplot domain. Classes are imposed on the seismic based on the model that defines these steps. A Classified section through the reservoir is shown in Figure 3, indicating pressure change only (light blue), low temperature (pink), moderate temperature (light red), and high temperature (dark red), as well as a cutoff to define the unaffected points (beige). The available temperature logs are overlain

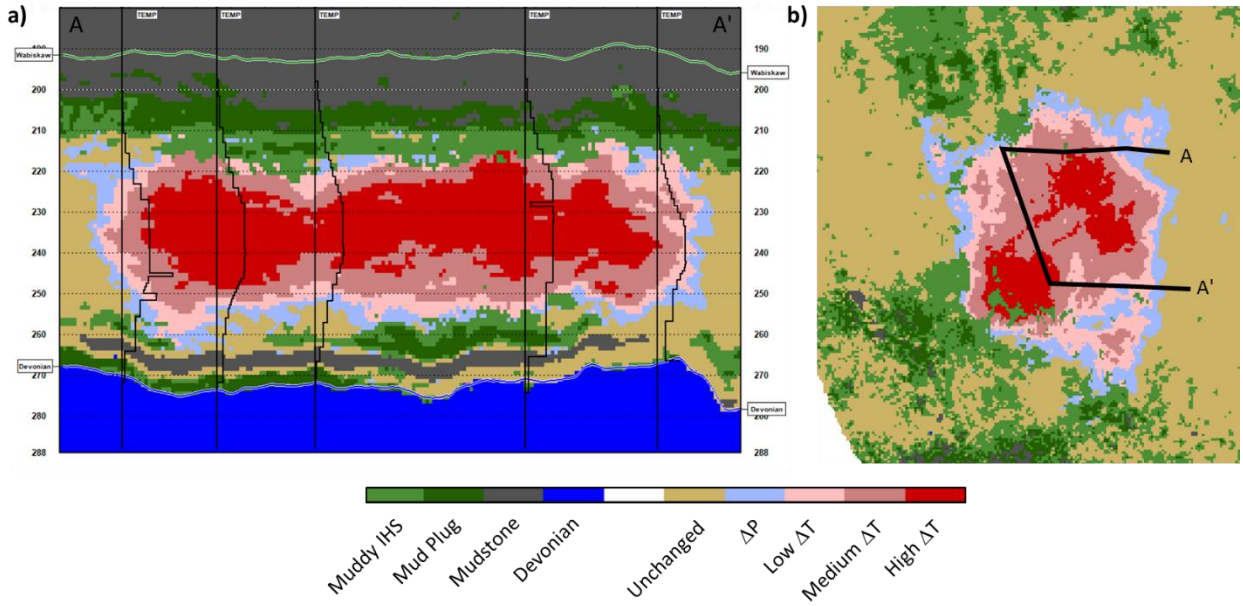

Figure 3. *a) Classified seismic section through the available temperature logs. The highest temperatures are in the centre of the reservoir above the level of the injectors (not shown). b) A horizon slice 30 ms below the Wabiskaw horizon showing the distribution of increased temperatures.*

on the classification and there is an excellent correspondence between the seismic classes and the logs. The hottest part of the reservoir is located in the centre of the steamed area, which falls above the horizontal wells.

Acknowledgements

We would like to thank CNOOC International Ltd. for permission to show the data.

References

Ciz, R., and S.A. Shapiro, 2007, Generalization of Gassmann equations for porous media saturated with a solid material: Geophysics, **72**, no. 6, A75-A79.

Dvorkin, J., and A. Nur, 1996, Elasticity of high-porosity sandstones: Theory for two North Sea data sets: Geophysics, **61**, 1363-1370.

Gray, F.D., K.A. Wagner, and D.J. Naidu, 2016, 3C-4D locates mobile bitumen in oil sands reservoirs: GeoConvention 2016, CSEG/CSPG/CWLS.

Hale, D., 2013, Dynamic warping of seismic images: Geophysics, **78**, no. 2, S105-S115.

Javanbakhti, A.R., 2018, Empirical modeling of the saturated shear modulus in heavy oil saturated rocks: Ph.D. Thesis, University of Calgary.

Maleki, M., A. Davolio, and D.J. Schiozer, 2018, Qualitative time-lapse seismic interpretation of Norne Field to assess challenges of 4D seismic attributes: The Leading Edge, **37**, 754-762.

Mesdag, P.R., M.R. Saberi, and C. Mangat, 2015, Updating the low-frequency model in time-lapse seismic inversion: A case study from a heavy-oil steam-injection project: The Leading Edge, **34**, 1456-1461.

Mutual, E., D. Cho, K. Innanen, 2017, Time-lapse rock physics inversion of thermal heavy oil production: 87th Annual Meeting, SEG, 585-589.

Nasser, M., D. Maguire, H.J. Hansen, and C. Schiott, 2016, Prestack 3D and 4D seismic inversion for reservoir static and dynamic properties: The Leading Edge, **35**, 415-422.